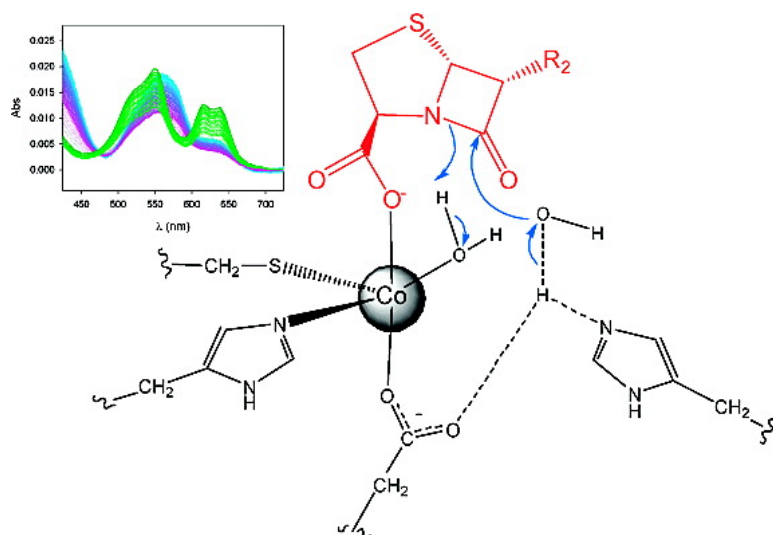


## Metal Content and Localization during Turnover in *B. cereus* Metallo- $\beta$ -lactamase

Leticia I. Llarrull, Mariana F. Tioni, and Alejandro J. Vila

*J. Am. Chem. Soc.*, **2008**, 130 (47), 15842-15851 • DOI: 10.1021/ja801168r • Publication Date (Web): 04 November 2008

Downloaded from <http://pubs.acs.org> on February 8, 2009



### More About This Article

Additional resources and features associated with this article are available within the HTML version:

- Supporting Information
- Access to high resolution figures
- Links to articles and content related to this article
- Copyright permission to reproduce figures and/or text from this article

[View the Full Text HTML](#)

## Metal Content and Localization during Turnover in *B. cereus* Metallo- $\beta$ -lactamase

Leticia I. Llarrull,<sup>†</sup> Mariana F. Tioni, and Alejandro J. Vila\*

*IBR (Instituto de Biología Molecular y Celular de Rosario), Consejo Nacional de Investigaciones Científicas y Técnicas de Argentina (CONICET), and Biophysics Section, Facultad de Ciencias Bioquímicas y Farmacéuticas, Universidad Nacional de Rosario, Suipacha 531, S2002LRK Rosario, Argentina*

Received February 15, 2008; E-mail: vila@ibr.gov.ar

**Abstract:** Metallo- $\beta$ -lactamases are enzymes capable of hydrolyzing all known classes of  $\beta$ -lactam antibiotics, rendering them ineffective. The design of inhibitors active against all classes of metallo- $\beta$ -lactamases has been hampered by the heterogeneity in metal content in the active site and the existence of two different mononuclear forms. BclI is a B1 metallo- $\beta$ -lactamase which is found in both mononuclear and dinuclear forms. Despite very elegant studies, there is still controversy on the nature of the active BclI species. We carried out a non-steady-state study of the hydrolysis of penicillin G catalyzed by Co(II)-substituted BclI, and we followed the modifications occurring at the active site of the enzyme. Working at different metal/enzyme ratios we demonstrate that both mono-Co(II) and di-Co(II) BclI are active metallo- $\beta$ -lactamases. Besides, we here present evidence that during penicillin G hydrolysis catalyzed by mono-Co(II) BclI the metal is localized in the DCH site (the Zn2 site in B1 enzymes). These conclusions allow us to propose that both in mono-Co(II) and di-Co(II) BclI the substrate is bound to the enzyme through interactions with the Co(II) ion localized in the DCH site. The finding that the DCH site is able to give rise to an active lactamase suggests that the Zn2 site is a common feature to all subclasses of metallo- $\beta$ -lactamases and would play a similar role. This proposal provides a starting point for the design of inhibitors based on transition-state analogs, which might be effective against all M $\beta$ LS.

### Introduction

The  $\beta$ -lactam antibiotic family represents the largest group of antibiotics within the antimicrobial weaponry used in the treatment of a variety of Gram-negative and Gram-positive infections.<sup>1</sup> It encompasses more than 50 marketed drugs, including the penicillins, cephalosporins, carbapenems, and monobactams, some of which have been used for more than six decades now.

Bacterial resistance is inevitably associated to antibiotic usage, being the natural outcome of the organism evolution to compete for survival.<sup>1</sup> Among different resistance mechanisms displayed by bacteria, the synthesis of  $\beta$ -lactamases is the most widely spread one.  $\beta$ -Lactamases are hydrolytic enzymes that selectively cleave the four-membered  $\beta$ -lactam ring, rendering antibiotics ineffective against their natural targets.<sup>1–3</sup> There are four molecular classes of  $\beta$ -lactamases known so far, namely, A–D, and include both metal-dependent (class B) and active-site serine (classes A, C, and D) enzymes.<sup>1,4</sup>

Metallo- $\beta$ -lactamases (M $\beta$ LS hereafter) are divided into three subclasses, B1, B2, and B3, all exhibiting resistance to com-

mercially available  $\beta$ -lactamase inhibitors.<sup>5–9</sup> This class of enzymes is of particular interest and concern owing to the ability of many of them to hydrolyze and, thus, provide resistance to virtually all classes of  $\beta$ -lactams, including the carbapenems. Most characterized M $\beta$ LS and all the plasmid-encoded ones fall within subclass B1.<sup>10</sup> All B1 lactamases are evolutionarily close to each other; despite a low level of sequence identity, they present the same fold and the metal ligands are fully conserved.<sup>5</sup> However, the finding of enzymes with different metal contents within this subclass has led to a strong debate about the metal ion occupancy and identity of the active species.<sup>11–17</sup>

<sup>†</sup> Current address: Department of Chemistry and Biochemistry, University of Notre Dame, Notre Dame, IN 46556.

- (1) Fisher, J. F.; Meroueh, S. O.; Mobashery, S. *Chem. Rev.* **2005**, *105* (2), 395–424.
- (2) Frere, J. M. *Mol. Microbiol.* **1995**, *16* (3), 385–395.
- (3) Perez, F.; Endimiani, A.; Hujer, K. M.; Bonomo, R. A. *Curr. Opin. Pharmacol.* **2007**, *7* (5), 459–469.
- (4) Ambler, R. P. *Philos. Trans. R. Soc. London (Biol)* **1980**, *289*, 321–331.

- (5) Crowder, M. W.; Spencer, J.; Vila, A. J. *Acc. Chem. Res.* **2006**, *39* (10), 721–728.
- (6) Walsh, T. R.; Toleman, M. A.; Poirel, L.; Nordmann, P. *Clin. Microbiol. Rev.* **2005**, *18* (2), 306–325.
- (7) Toney, J. H.; Moloughney, J. G. *Curr. Opin. Investig. Drugs* **2004**, *5* (8), 823–826.
- (8) Bebrone, C. *Biochem. Pharmacol.* **2007**, *74* (12), 1686–1701.
- (9) Cricco, J. A.; Rasia, R. M.; Orellano, E. G.; Ceccarelli, E. A.; Vila, A. J. *Coord. Chem. Rev.* **1999**, *190–192*, 519–535.
- (10) Hall, B. G.; Salipante, S. J.; Barlow, M. J. *Mol. Evol.* **2003**, *57* (3), 249–254.
- (11) de Seny, D.; Heinz, U.; Wommer, S.; Kiefer, M.; Meyer-Klaucke, W.; Galleni, M.; Frere, J. M.; Bauer, R.; Adolph, H. W. *J. Biol. Chem.* **2001**, *276* (48), 45065–45078.
- (12) Paul-Soto, R.; Bauer, R.; Frere, J. M.; Galleni, M.; Meyer-Klaucke, W.; Nolting, H.; Rossolini, G. M.; de Seny, D.; Hernandez-Valladares, M.; Zeppezauer, M.; Adolph, H. W. *J. Biol. Chem.* **1999**, *274* (19), 13242–13249.
- (13) Badarau, A.; Dambon, C.; Page, M. I. *Biochem. J.* **2007**, *401*, 197–203.
- (14) Badarau, A.; Page, M. I. *Biochemistry* **2006**, *45* (36), 11012–11020.

The first crystal structure solved for an M $\beta$ L was that of BcII from *Bacillus cereus*, which contained one Zn(II) ion in the active site bound to three His residues (His116, His118, and His196)<sup>18</sup> and a H<sub>2</sub>O/OH<sup>-</sup> molecule in the so-called Zn1 or 3H site.<sup>19</sup> Subsequent structures of BcII and other B1 enzymes revealed that they are able to host a dinuclear metal center containing the tetrahedral 3H site and an additional trigonal bipyramidal Zn(II) site (the Zn2 or DCH site), where the metal ion is coordinated to Asp120, Cys221, His263, a bridging H<sub>2</sub>O/OH<sup>-</sup>, and an additional water molecule (Figure 1A).<sup>20–22</sup> These findings suggested the possible existence of two active species with different metal content: the mononuclear and dinuclear forms of BcII, which could display distinct catalytic mechanisms.

Different spectroscopic studies in solution later questioned the identity of the mono-Zn(II) form observed in the crystallographic studies. It was shown that when one equivalent of Zn(II), Co(II), or Cd(II) is added to apo-BcII, a mixture of different monometallic species is formed that were shown to be in equilibrium in some cases.<sup>11,12,15,16</sup> This picture has prevented any straightforward interpretation of the activity data of monometallic species.

Different reports of kinetic studies of BcII with variable metal contents are available.<sup>11–14,22–26</sup> However, they have been carried out in different experimental conditions, and (most worrying) the metal content and localization of the metal ions was not addressed in most of these cases. This has been hampered mainly by two reasons: (1) the lack of metal binding constants measured in the same conditions in which the kinetic studies have been performed and (2) the difficulty in assessing the location of the metal ions between the two binding sites in the resting-state enzyme and during turnover.

Zn(II) is a d<sup>10</sup> metal ion, silent to most spectroscopic techniques. High-spin Co(II), instead, is an adequate surrogate for Zn(II) in metalloenzymes since it is able to display similar catalytic performances and structural features.<sup>27</sup> We and others have extensively exploited Co(II) substitution in M $\beta$ Ls to probe the metal site in the resting state<sup>15,22,28–33</sup> and, relevant to this

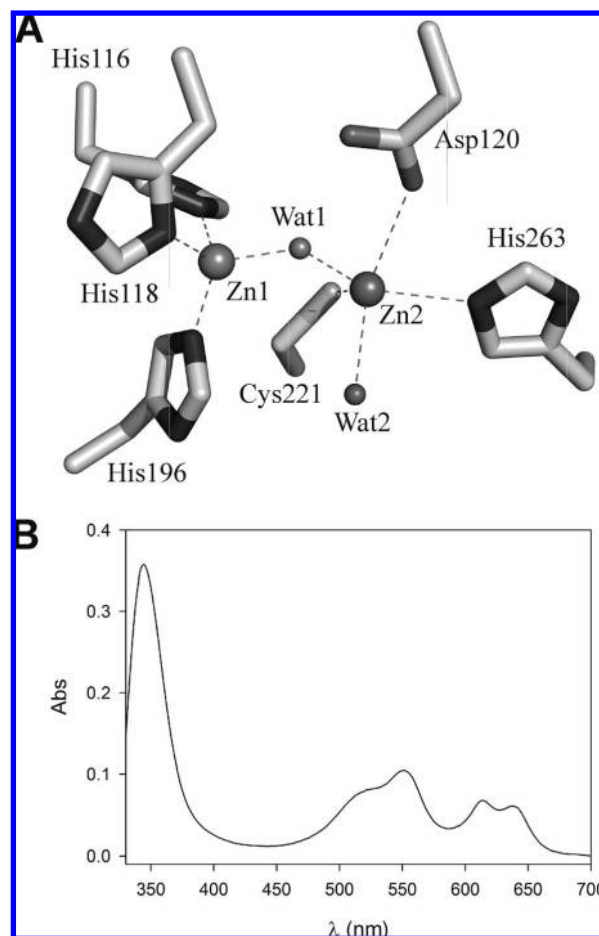


**Figure 1.** (A) Dinuclear Zn(II) site observed in BcII; figure rendered with PyMol (DeLano Scientific LLC) from Protein Data Bank file 1bc2. (B) Electronic spectrum of di-Co(II) BcII recorded in 100 mM HEPES pH 7.5, 200 mM NaCl. The spectrum of apo-BcII was subtracted from the spectrum of di-Co(II) BcII.

work, during turnover.<sup>34–37</sup> Among them, it is worth mentioning a series of elegant studies in this area reported by Bicknell, Waley, and co-workers two decades ago on Co(II)-substituted BcII.<sup>34,35</sup> These authors documented the accumulation of two different intermediates during turnover by electronic and MCD spectroscopy and proposed a branched mechanism for penicillin G hydrolysis by Co(II)–BcII. These pioneering studies were carried out with excess Co(II) in the reaction milieu, i.e., in experimental conditions that cannot be employed to evaluate the contribution of mono-Co(II) BcII to the catalytic mechanism. In addition, those experiments were performed before the availability of a crystal structure for BcII and therefore

- (15) Llarrull, L. I.; Tioni, M. F.; Kowalski, J.; Bennett, B.; Vila, A. J. *J. Biol. Chem.* **2007**, *282* (42), 30586–30595.
- (16) Henningsen, L.; Dambon, C.; Antony, J.; Jensen, M.; Adolph, H. W.; Wommer, S.; Roberts, G. C.; Bauer, R. *J. Am. Chem. Soc.* **2001**, *123* (42), 10329–10335.
- (17) Wommer, S.; Rival, S.; Heinz, U.; Galleni, M.; Frere, J. M.; Franceschini, N.; Amicosante, G.; Rasmussen, B.; Bauer, R.; Adolph, H. W. *J. Biol. Chem.* **2002**, *277* (27), 24142–24147.
- (18) Galleni, M.; Lamotte-Brasseur, J.; Rossolini, G. M.; Spencer, J.; Dideberg, O.; Frere, J. M. *Antimicrob. Agents Chemother.* **2001**, *45* (3), 660–663.
- (19) Carfi, A.; Pares, S.; Duee, E.; Galleni, M.; Duez, C.; Frère, J. M.; Dideberg, O. *EMBO J.* **1995**, *14*, 4914–4921.
- (20) Fabiane, S. M.; Sohi, M. K.; Wan, T.; Payne, D. J.; Bateson, J. H.; Mitchell, T.; Sutton, B. J. *Biochemistry* **1998**, *37*, 12404–12411.
- (21) Concha, N.; Rasmussen, B. A.; Bush, K.; Herzberg, O. *Structure* **1996**, *4*, 823–836.
- (22) Orellano, E. G.; Girardini, J. E.; Cricco, J. A.; Ceccarelli, E. A.; Vila, A. J. *Biochemistry* **1998**, *37*, 10173–10180.
- (23) Bounaga, S.; Laws, A. P.; Galleni, M.; Page, M. I. *Biochem. J.* **1998**, *31*, 703–711.
- (24) Rasia, R. M.; Vila, A. J. *Biochemistry* **2002**, *41* (6), 1853–1860.
- (25) Badarau, A.; Page, M. I. *Biochemistry* **2006**, *45* (35), 10654–10666.
- (26) de Seny, D.; Prosperi-Meys, C.; Bebrone, C.; Rossolini, G. M.; Page, M. I.; Noel, P.; Frere, J. M.; Galleni, M. *Biochem. J.* **2002**, *363* (Pt 3), 687–696.
- (27) Bertini, I.; Luchinat, C. *Adv. Inorg. Biochem.* **1985**, *6*, 71–111.
- (28) Rasia, R. M.; Ceolin, M.; Vila, A. J. *Protein Sci.* **2003**, *12* (7), 1538–1546.
- (29) Llarrull, L. I.; Fabiane, S. M.; Kowalski, J. M.; Bennett, B.; Sutton, B. J.; Vila, A. J. *J. Biol. Chem.* **2007**, *282* (25), 18276–18285.

- (30) Tomatis, P. E.; Rasia, R. M.; Segovia, L.; Vila, A. J. *Proc. Natl. Acad. Sci. U. S. A.* **2005**, *102* (39), 13761–13766.
- (31) Periyannan, G. R.; Costello, A. L.; Tierney, D. L.; Yang, K. W.; Bennett, B.; Crowder, M. W. *Biochemistry* **2006**, *45* (4), 1313–1320.
- (32) Davies, R. B.; Abraham, E. P. *Biochem. J.* **1974**, *143*, 129–135.
- (33) Hernandez, V. M.; Kiefer, M.; Heinz, U.; Soto, R. P.; Meyer-Klaucke, W.; Nolting, H. F.; Zeppezauer, M.; Galleni, M.; Frere, J. M.; Rossolini, G. M.; Amicosante, G.; Adolph, H. W. *FEBS Lett.* **2000**, *467* (2–3), 221–225.
- (34) Bicknell, R.; Schaeffer, A.; Waley, S. G.; Auld, D. S. *Biochemistry* **1986**, *25*, 7208–7215.
- (35) Bicknell, R.; Waley, S. G. *Biochemistry* **1985**, *24*, 6876–6887.
- (36) Sharma, N. P.; Hajdin, C.; Chandrasekar, S.; Bennett, B.; Yang, K. W.; Crowder, M. W. *Biochemistry* **2006**, *45* (35), 10729–10738.
- (37) Garrity, J. D.; Bennett, B.; Crowder, M. W. *Biochemistry* **2005**, *44* (3), 1078–1087.

interpreted by assuming a single metal binding site. Lately, Badarau and Page suggested that di-Co(II) BcII is the only active species.<sup>14</sup>

We recently determined the macroscopic dissociation constants of the different Co(II) binding sites in BcII and assessed the metal distribution by exploiting different spectroscopic techniques.<sup>15</sup> We demonstrated that mono-Co(II) and di-Co(II) BcII coexist at Co(II)/BcII ratios < 1 and that mono-Co(II) BcII is a mixture of two enzyme populations, one with metal bound in the 3H site and another one with Co(II) bound in the DCH site. With this information in hand we decided to carry out a non-steady-state kinetic and spectroscopic study of the hydrolysis of penicillin G by Co(II)-substituted BcII with different metal contents. These studies allow us to demonstrate that (1) both mono-Co(II) and di-Co(II) BcII species are active and (2) an active mono-Co(II) species accumulates at low Co(II)/BcII ratios which contains the metal ion localized in the DCH site, contradicting the canonical expectation that in mononuclear B1 lactamases the catalytic site is the 3H site. These results suggest that new strategies for inhibitor design should be envisaged.

## Experimental Section

**Reagents.** All chemicals were of the highest quality available. *E. coli* BL21(DE3)pLysS' cells (Stratagene, CA) were employed for protein production. Luria–Bertani (LB) medium (Sigma) was used as the growth media for all bacterial strains.

**Enzyme Expression and Purification.** Wild-type BcII was expressed in *E. coli* BL21(DE3)pLysS' as a fusion protein with glutathione-S-transferase and purified as previously described.<sup>15,22</sup> The purity of the enzyme preparations was checked by SDS-PAGE. Protein concentration was measured spectrophotometrically using  $\epsilon_{280} = 30\,500\text{ M}^{-1}\text{ cm}^{-1}$ .<sup>12</sup> Metal content in protein samples was checked using the colorimetric reagent PAR<sup>38</sup> and ranged between 1.4 and 1.8 metal/total protein depending on the enzyme preparation.

**Metal Derivatives.** All buffer solutions used to prepare the apoenzyme were treated by extensive stirring with Chelex 100 (Sigma). Apo-BcII was prepared by dialysis of the purified holo-protein (approximately 200  $\mu\text{M}$ ) against two changes of >100 volumes of 10 mM HEPES pH 7.5, 0.2 M NaCl, 20 mM EDTA over a 12 h period. EDTA was removed from the resulting apoenzyme solution by three dialysis steps against >100 volumes of 10 mM HEPES pH 7.5, 1 M NaCl, 0.3 g/L Chelex 100, one dialysis step against >100 volumes of 10 mM HEPES pH 7.5, 0.2 M NaCl, 0.3 g/L Chelex 100, and finally two dialysis steps against >100 volumes of 10 mM HEPES pH 7.5, 0.2 M NaCl, 0.3 g/L Chelex 100. All dialysis steps were carried out at 4 °C under stirring and for at least 6 h. Metal content in apoprotein samples was checked using the colorimetric reagent PAR.

A solution of 200–300  $\mu\text{M}$  apo-BcII in 100 mM HEPES pH 7.5, 0.2 M NaCl was titrated with a 10.6 mM CoSO<sub>4</sub> stock solution prepared in 100 mM HEPES pH 7.5, 0.2 M NaCl. Spectra were recorded at room temperature in a Jasco 550 UV–vis spectrophotometer. The spectra were corrected for dilution on adding Co(II), and the UV–vis difference spectra were obtained by subtracting the spectrum of apo-BcII. Complete formation of the di-Co(II) adduct, as monitored by UV–vis spectroscopy, was achieved at a ratio of 1.4–1.8 Co(II)/total protein, depending on the enzyme preparation. In all preparations the level of Co(II) uptake of the apo-enzymes paralleled the original Zn(II) content of the protein as isolated. The concentration of “metallable” protein was calculated as already described.<sup>15</sup> Co(II) was added to apoprotein samples of known concentration of “metallable” protein to obtain samples with different Co(II)/BcII ratios: 0.3, 1, and 2.

**Stopped-Flow Experiments.** The variations in the visible spectra of Co(II) derivatives of BcII during hydrolysis of penicillin G were followed with an Applied Photophysics SX.18-MVR stopped-flow system associated to a photodiode-array detector (Applied Photophysics, U.K.). The measurements were performed in 100 mM Hepes, pH 7.5, 0.2 M NaCl, at 6 °C. The data were corrected for the instrument dead time (2 ms). A set of scans was acquired in the wavelength range of 300–730 nm, with 1.28 ms integration time, during hydrolysis of penicillin G solutions (0.5, 2.5, and 20 mM) in 100 mM Hepes, pH 7.5, 0.2 M NaCl catalyzed by BcII samples (~100  $\mu\text{M}$ ) with different Co(II) concentrations.

**Kinetic Analysis of the Stopped-Flow Data.** Nonlinear regression analysis was used to fit the single-wavelength traces with the program Dynafit (BioKin).<sup>39</sup> The concentrations of the different metal-loaded species in the sample (apo, mono-Co(II), di-Co(II), and tri-Co(II) BcII) were calculated based on the concentration of enzyme capable of binding metal as determined from the Co(II) titration of the apoprotein and on the previously determined Co(II) dissociation constants ( $K_{D1} = 0.10\ \mu\text{M}$ ,  $K_{D2} = 0.17\ \mu\text{M}$ , and  $K_{D3} = 94\ \mu\text{M}$ ).<sup>15</sup> We assumed that the mixing time in the stopped-flow equipment was too short for the metal-loaded species to re-equilibrate upon dilution of the protein sample with substrate (1:1 ratio). This assumption is consistent with the estimated Co(II) dissociation rates.<sup>11,15</sup> The concentrations of the different metal-loaded species in the syringe prior to mixing with substrate were calculated with the program DynaFit, and the results are shown in Table S1 (Supporting Information). In all cases, the concentration of the tri-Co(II) species was low enough and could be neglected in the kinetic models. The initial concentrations of the different metal-loaded species in the reaction were estimated as one-half the concentration of the corresponding species in the enzyme syringe, taking into account the dilution upon mixing with substrate (1:1 mixture) (Table S1, Supporting Information).

The program DynaFit employs rate constants for the numerical fits. Hence, when the equilibria between apo-, mono-, and di-Co(II) BcII were included in the kinetic models, the corresponding equilibria were described as a combination of two rate constants ( $K_D = k_{\text{off}}/k_{\text{on}}$ ). The rate constants corresponding to binding of Co(II) were fixed to the values informed by Seny et al.:  $k_{\text{on1}} = 0.28\ \mu\text{M}^{-1}\cdot\text{s}^{-1}$  and  $k_{\text{on2}} = 0.03\ \mu\text{M}^{-1}\cdot\text{s}^{-1}$ .<sup>11</sup> The values of  $k_{\text{off}}$  were calculated based on the corresponding metal dissociation constants ( $K_{D1}$  and  $K_{D2}$ ) and the  $k_{\text{on}}$  values. The calculated  $k_{\text{off}}$  values were  $k_{\text{off1}} = 0.028\ \text{s}^{-1}$  and  $k_{\text{off2}} = 0.005\ \text{s}^{-1}$ .

## Results

**Stopped-Flow/Photodiode Array Experiments.** In order to identify the catalytically relevant metal-loaded BcII species, we followed the hydrolysis of penicillin G catalyzed by BcII samples with different Co(II)/BcII ratios using a stopped-flow system associated to a photodiode array detector. The experiments were performed at 6 °C in the same buffer employed for determination of the metal dissociation constants (Hepes pH 7.5, 200 mM NaCl).

Di-Co(II) BcII has a Cys → Co(II) LMCT band at 343 nm attributed to the DCH site and a pattern of ligand field bands (with maxima at 530, 550, 615, and 640 nm) which is mainly due to the metal ion localized in the 3H site (Figure 1B).<sup>11,15,22,32</sup> The electronic spectrum of di-Co(II) BcII changes during turnover, as shown for hydrolysis of a solution of 20 mM penicillin G (Figure 2). A differential analysis of the spectra registered during turnover allows detection of three well-defined steps along the reaction. Thus, monitoring the absorption features of the metal site is more informative than following exclusively substrate hydrolysis or product formation and allows obtention of the individual rate constants of these steps.

(38) Hunt, J. B.; Neece, S. H.; Ginsburg, A. *Anal. Biochem.* **1985**, *146* (1), 150–157.

(39) Kuzmic, P. *Anal. Biochem.* **1996**, *237*, 260–273.



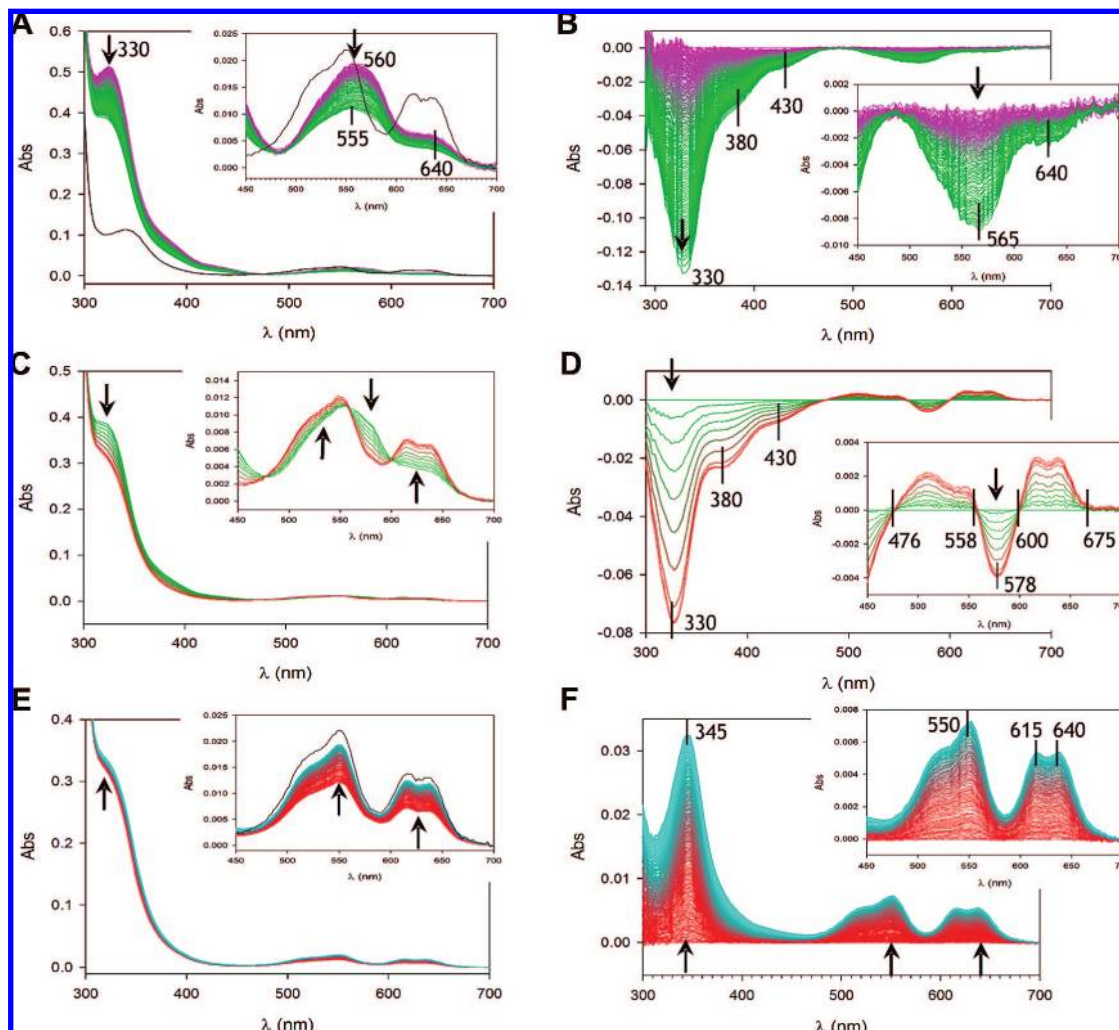


**Figure 2.** Photodiode array stopped-flow spectra of di-Co(II) BcII (main species at 64.5  $\mu$ M enzyme with 3 Co(II) equivalents) during the hydrolysis of 20 mM penicillin G in 100 mM HEPES pH 7.5, 200 mM NaCl, at 6  $^{\circ}$ C. (A) Spectral changes corresponding to the decay of ES<sup>1</sup> between 0.002 (purple) and 6 s (green) after mixing during conversion to the ES<sup>2</sup> complex. (B) Difference spectra corresponding to the spectra shown in A, recorded in the time interval from 0.002 (purple) to 6 s (green) after mixing, which were obtained by subtraction of the spectrum recorded 0.002 s after mixing (initial time of the phase). (C) Spectral changes corresponding to the recovery of resting enzyme E from ES<sup>1</sup> between 6 (green) and 7 s (red) after mixing. (D) Difference spectra corresponding to the spectra shown in C, recorded in the time interval from 6 (green) to 7 s (red) after mixing, which were obtained by subtraction of the spectrum recorded 6 s after mixing. (E) Spectral changes corresponding to recovery of resting enzyme E from ES<sup>2</sup> between 7 (red) and 50 s (cyan) after mixing. (F) Difference spectra corresponding to the spectra shown in C, recorded in the time interval from 7 (red) to 50 s (cyan) after mixing, which were obtained by subtraction of the spectrum recorded 7 s after mixing. In A–F, the insets show an amplification of the ligand field bands (in the 450–700 nm region of the spectra). The arrows indicate whether there is an increase or a decrease in the intensity of the corresponding absorption bands. Formation of ES<sup>1</sup> from resting enzyme takes place in the dead time of the equipment and cannot be detected. The difference spectrum obtained upon subtraction of the corresponding spectra of resting BcII from the first spectra recorded after the dead time of the equipment shows similar features (but opposite in sign, as expected) compared to those in Figure 2D.

The first spectrum recorded after the instrument dead time ( $\sim$ 0.002 s) differs from that of the resting state enzyme, and presents an intense absorption band at 330 nm and a pattern of ligand-field bands between 480–670 nm, with maxima at 560 and 640 nm (Figure 2A). This species is named ES<sup>1</sup>, following the labeling scheme used in previous studies.<sup>34,35</sup> After fast accumulation of ES<sup>1</sup>, a second phase is observed (from 0.002 to 6 s) where the intensities of the 330, 560 and 640 nm bands decrease (Figure 2A/B). This phase was attributed to conversion of ES<sup>1</sup> into a second intermediate, with lower absorptivity, named ES<sup>2</sup>. From 6 to 7 s, ES<sup>1</sup> converts to resting enzyme (Figure 2C). The difference spectra presented isosbestic points at 476, 558, 600 and 675 nm (Figure 2D). The last phase observed (from 7 to 50 s) evidenced the recovery of the resting enzyme from a species with absorption bands of lower intensity, tentatively ES<sup>2</sup> (Figure 2E/F). This last phase could not be

detected on assays carried out at lower substrate concentrations (0.5 and 2.5 mM), presumably due to a lower extent of accumulation of ES<sup>2</sup>.

The same reaction was run using BcII samples substituted with different Co(II)/enzyme ratios. Table S1 (Supporting Information) lists the equilibrium concentrations of the metal-loaded species present at different Co(II)/BcII ratios based on the already reported binding constants of Co(II) to apo-BcII under these conditions.<sup>15</sup> The time evolution of the spectra during turnover was similar at the different Co(II) contents assayed. Indeed, the spectrum of the first intermediate detected after the dead time of the equipment seemed to be the same regardless of the Co(II) concentration (Figure S1, Supporting Information) and the same protein species seemed to be involved during turnover (Figure 3) despite the different populations of the metallated forms before mixing (Table S1, Supporting

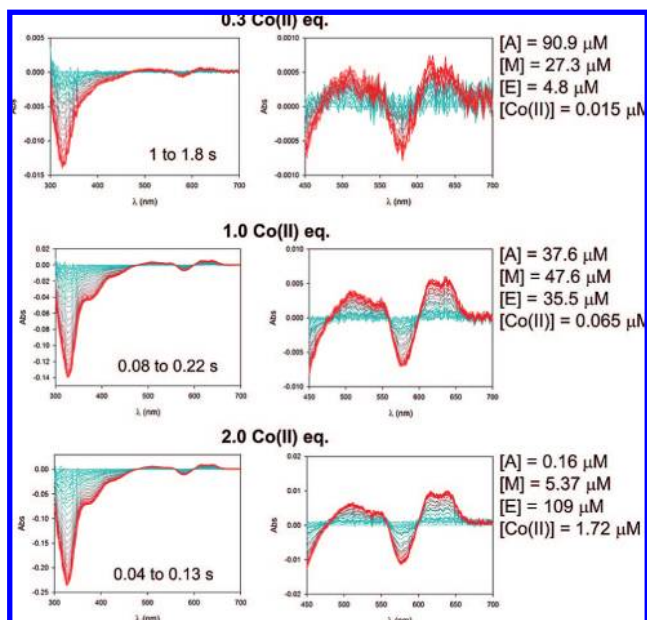


**Figure 3.** Difference spectra corresponding to conversion of  $ES^1$  or  $MS$  to  $E$  or  $M$ , depending on the  $Co(II)/BcII$  ratio, recorded during reaction of 0.5 mM penicillin G with 123  $\mu M$  BcII substituted with 0.3, 1, and 2  $Co(II)$  equivalents (eq.). The difference spectra were obtained by subtraction of the spectrum recorded at the lower time in the time interval (cyan, shorter time; red, longer time). In each case, on the right we show an amplification of the ligand field bands region (450–700 nm). The concentrations of the different enzyme species present in each enzyme sample in resting state were calculated based on the  $Co(II)$  dissociation constant and are listed on the right: A, apo-BcII; M, mono- $Co(II)$  BcII; and E, di- $Co(II)$  BcII.

Information). The simplest explanation to these observations is to assume that di- $Co(II)$  BcII is the only active species, as proposed by Badarau and Page.<sup>14</sup> Under this hypothesis, the observed  $ES^1$  complex would hold a dinuclear  $Co(II)$  center.

**Kinetic Analysis of the Reaction of  $Co(II)$ –BcII and Penicillin G.** We analyzed the spectra corresponding to the different species observed during turnover and identified three wavelength values where the most significant changes were observed (330, 578, and 640 nm) (Figure 2). The band at 343 nm in the resting state  $Co(II)$ –BcII is a Cys221  $\rightarrow$   $Co(II)$  CT band that is shifted to 330 nm, increasing its intensity. This absorption band can be exploited as a probe of the DCH site during the reaction. The absorption features in the visible range in resting state  $Co(II)$ –BcII correspond mostly to ligand field absorptions from the 3H site. The intermediate species  $ES^1$  presented a different pattern of d–d bands with maxima at 560 and 640 nm, which can correspond to either the 3H or the DCH site or to the additive contribution of both sites. The spectral changes in the visible region can thus be monitored through the absorption at different wavelengths. We decided to monitor the absorption band at 578 nm, which has the largest absorption difference between the spectra of  $ES^1$  and  $E$  while showing at the same time a significant difference between the spectra of  $ES^1$  and  $ES^2$ .

We followed the changes in the electronic spectra of the enzyme upon hydrolysis of penicillin G (0.5 and 2.5 mM) catalyzed by 123  $\mu M$  BcII substituted with 1 or 2  $Co(II)$  equivalents. We initially fitted the time evolution of the absorption at 578 nm, which (in contrast to the LMCT band at 330 nm) displays no interference due to substrate or product absorption. We fitted simultaneously the variations of the 578 nm absorption registered at the four experimental conditions

by nonlinear regression analysis. The concentrations of the different metal-loaded species in the sample were calculated based on the previously determined  $Co(II)$  dissociation constants (Table S1, Supporting Information).<sup>15</sup>

We initially evaluated branched models that assumed that di- $Co(II)$  BcII is the only active species (see Models I and II in Scheme 1). Neither of these models allowed us to fit simultaneously the traces corresponding to BcII substituted with 1 and 2  $Co(II)$  equivalents (Figure S2 and S3, Supporting Information). For reactions run with 1  $Co(II)/BcII$ , these models predicted much lower reaction rates than observed. This reveals that assuming that di- $Co(II)$  BcII is the only active species does not provide an adequate description of the enzyme behavior at substoichiometric metal contents.

Hence, we evaluated different models which considered mono- $Co(II)$  BcII as an additional active species. The best fit of the stopped-flow data was obtained with Model III (Scheme 1), where mono- $Co(II)$  BcII can bind substrate to give rise to a catalytically competent enzyme–substrate complex ( $MS$ ) which also absorbs at 578 nm (cf. Figure 4A and Table 1). This model requires the existence of three enzyme–substrate complexes: the dinuclear adducts  $ES^1$  and  $ES^2$  and the mononuclear adduct  $MS$ . The model also includes the already existing equilibria between apo, mono- $Co(II)$ , and di- $Co(II)$  BcII, described by independently determined constants.<sup>11,15</sup>

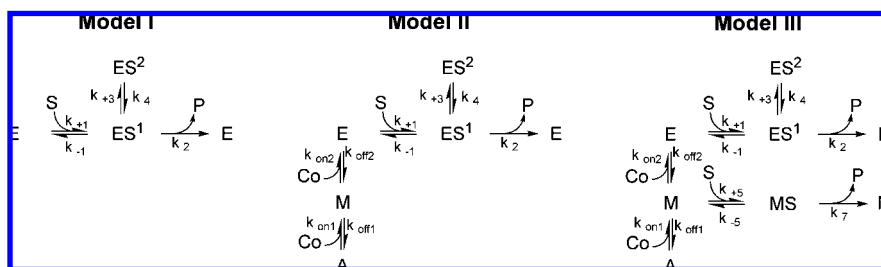
We also evaluated some variations to Model III, aimed at reducing the number of enzyme–substrate complexes involved, e.g., by assuming that metal dissociation from  $ES^1$  could give rise to free mono- $Co(II)$  BcII ( $M$ ) or to the mononuclear enzyme–substrate complex  $MS$  (Models IV and V, respectively, see Figures S4 and S5, Supporting Information). Neither of these models provided a satisfactory fit together with a set of reliable constants. In addition, it is unlikely that a dinuclear BcII–substrate adduct can release one metal ion once the substrate is bound. On the basis of these observations, Model III stands as the best minimal model able to describe the experimental data. As detailed in Table 1, some parameters were fixed or independently determined.

**Assessing the Metal Ion Localization.** The spectroscopic data available for the resting enzyme indicate that mono- $Co(II)$  BcII is a mixture of at least two populations (mono- $Co(II)$ •3H and mono- $Co(II)$ •DCH).<sup>15</sup> Therefore, it remains to clarify the metal localization in the active  $MS$  intermediate. The different d–d bands observed during turnover can be attributed to either the 3H or DCH site; instead, the LMCT bands are a fingerprint of the DCH site. In order to address the identity of the active  $MS$  species, we fitted the changes observed in the Cys  $\rightarrow$   $Co(II)$  charge-transfer band at 330 nm to the same models previously described. The best fit was also achieved with Model III (Scheme 1 and Figure 4B). The constants obtained from the fit of the absorption at 330 nm are in excellent agreement with the values obtained from the independent fit of the 578 nm band to the same model (Table 1), revealing the robustness of the proposed model.

Model III assumes that all the population of free mono- $Co(II)$  BcII ( $M$ ) gives rise to a unique  $MS$  adduct, which displays a LMCT band at 330 nm. The assumption of a single mononuclear enzyme–substrate intermediate implies that the  $Co(II)$  ion is localized in the DCH site in this enzyme–substrate adduct.

(40) Rasia, R. M.; Vila, A. J. *J. Biol. Chem.* **2004**, *279* (25), 26046–26051.  
(41) Spencer, J.; Clarke, A. R.; Walsh, T. R. *J. Biol. Chem.* **2001**, *276* (36), 33638–33644.

## Scheme 1



Alternatively, we evaluated the possibility that both mononuclear species were active (Figure S9, Supporting Information) assuming a 1:1 ratio of mono-Co(II)·3H and mono-Co(II)·DCH (the microscopic dissociation constants for these species are not known). In contrast to Model III, the best fit obtained using this model gives rise to different rate constants when the data at 330 and 578 nm are independently analyzed. However, this inconsistency could be due to the assumptions and simplifications involved in this complex model. Thus, our data indicate that mono-Co(II)·DCH BcII is active, but we cannot rule out the possibility that mono-Co(II)·3H BcII is also active.

## Discussion

The mechanism and identity of the catalytically relevant species of metallo- $\beta$ -lactamases in general and of BcII in particular have been extensively studied.<sup>11–14,22–25,42</sup> Elucidation of both issues is essential for any attempt of rational inhibitor design which should target the different active species. Wommer and co-workers suggested that BcII achieves its maximal efficiency with one bound Zn(II) ion,<sup>17</sup> while Badarau and Page recently proposed that di-Co(II)–BcII is the only active species.<sup>14</sup> At low metal/BcII ratios, a mixture of apo, monometallic, and dimetallic species coexist in equilibrium in the reaction milieu, thus making it difficult to assess the specific activity of each metal-loaded species.<sup>15</sup> Thus far, most steady-state kinetic studies have overlooked this issue. Most important, these studies have been limited by the difficulty in assessing the location of the metal ions between the two binding sites in the resting-state enzyme and during turnover. In addition, many of these studies were performed in the presence of excess Co(II). Under these conditions, the predominant enzyme species are

di-Co(II) and tri-Co(II) BcII.<sup>15</sup> On the basis of the Co(II) dissociation constants which we recently determined, we designed stopped-flow experiments under conditions where the predominant species are mono-Co(II) and di-Co(II) BcII. We studied the hydrolysis of the  $\beta$ -lactam antibiotic penicillin G catalyzed by the enzyme BcII substituted with different Co(II)/enzyme ratios.

The stopped-flow experiments followed using a photodiode array show that penicillin G hydrolysis by Co(II)–BcII proceeds by way of a branched kinetic mechanism, in agreement with the model proposed by Bicknell et al. for BcII with excess Co(II) at pH 6 (Model I, Scheme 1).<sup>34,35</sup> The absence of structural data available at that time precluded an accurate description of the catalytic mechanism of BcII. Despite this fact, that report still stands as one of the most elegant studies on  $M\beta L$ -mediated hydrolysis. We found that this branched mechanism is unable to account for the catalytic behavior of BcII at substoichiometric Co(II)/BcII ratios, and here we provide strong evidence that both di-Co(II) and mono-Co(II) BcII are active.

The electronic spectra of the intermediate that accumulates after the dead time of the experiment are identical for all assayed Co(II)/BcII ratios (Figure S1, Supporting Information). This observation would support the proposal that there is only one active species, namely, di-Co(II) BcII. However, the data recorded upon hydrolysis of penicillin G with different Co(II)/BcII ratios cannot be fitted simultaneously to Model I or II. Both models assume that di-Co(II) BcII is the only active species, and Model II also includes the equilibria between the different metal-loaded forms of resting-state BcII (i.e., the possibility that these equilibria are being shifted toward the di-Co(II) form upon substrate binding). The possibility that two

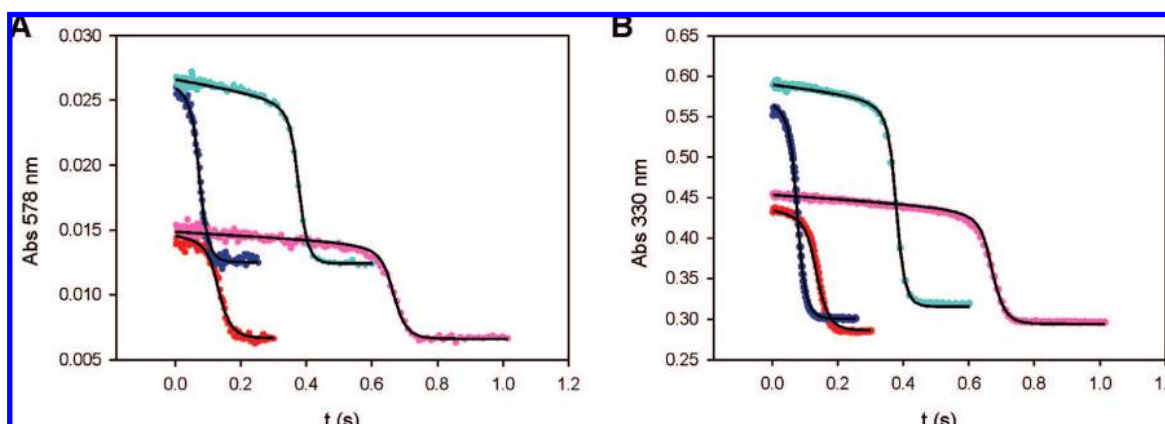


**Figure 4.** Fit of the changes in the intensity of the absorption bands with time to Model III. (A and B) Traces at 578 and 330 nm, respectively. The experimental points (dotted lines) are shown overlapped with the fitted curves (solid lines). In every case 123  $\mu$ M BcII was used. The different traces in each graph correspond to reaction of BcII substituted with 1 Co(II) equivalent and 0.5 mM penicillin G (red dots), BcII substituted with 1 Co(II) equivalent and 2.5 mM penicillin G (pink dots), BcII substituted with 2 Co(II) equivalents and 0.5 mM penicillin G (blue dots), and BcII substituted with 2 Co(II) equivalents and 2.5 mM penicillin G (cyan dots).



**Table 1.** Parameters Obtained from the Fits of the Changes in the Intensity of Absorption at 578 and 330 nm, Corresponding to the Reaction of Co(II)-Substituted BcII with Penicillin G, with Model III (Scheme 1)<sup>a</sup>

	578 nm	330 nm
$k_{+1}$ ( $\mu\text{M}^{-1}\cdot\text{s}^{-1}$ )	6.5 (0.6)	4.5 (0.2)
$k_{-1}$ ( $\text{s}^{-1}$ )	90 (10)	31 (5)
$k_2$ ( $\text{s}^{-1}$ )	64.3 (0.3)	62.7 (0.2)
$k_{+3}$ ( $\text{s}^{-1}$ )	0.30 (0.02)	0.19 (0.02)
$k_4$ ( $\text{s}^{-1}$ ) <sup>b</sup>	0.018 (fixed)	0.018 (fixed)
$k_{+5}$ ( $\mu\text{M}^{-1}\cdot\text{s}^{-1}$ ) <sup>c</sup>	7 (fixed)	7 (fixed)
$k_{-5}$ ( $\text{s}^{-1}$ ) <sup>c</sup>	80 (fixed)	80 (fixed)
$k_7$ ( $\text{s}^{-1}$ )	37.1 (0.2)	36.1 (0.2)
$k_{\text{on}1}$ ( $\mu\text{M}^{-1}\cdot\text{s}^{-1}$ )	0.28 (fixed)	0.28 (fixed)
$k_{\text{off}1}$ ( $\text{s}^{-1}$ )	0.028 (fixed)	0.028 (fixed)
$k_{\text{on}2}$ ( $\mu\text{M}^{-1}\cdot\text{s}^{-1}$ )	0.03 (fixed)	0.03 (fixed)
$k_{\text{off}2}$ ( $\text{s}^{-1}$ )	0.005 (fixed)	0.005 (fixed)
$r_{\text{M}}$ ( $\text{M}^{-1}\cdot\text{cm}^{-1}$ )	56.6 (0.9)	4080 (10)
$r_{\text{MS}}$ ( $\text{M}^{-1}\cdot\text{cm}^{-1}$ )	134.3 (0.6)	5440 (10)
$r_{\text{E}}$ ( $\text{M}^{-1}\cdot\text{cm}^{-1}$ )	113.0 (0.5)	2534 (6)
$r_{\text{ES}1}$ ( $\text{M}^{-1}\cdot\text{cm}^{-1}$ )	240.0 (0.4)	5031 (9)
$r_{\text{ES}2}$ ( $\text{M}^{-1}\cdot\text{cm}^{-1}$ )	100 (7)	5000 (200)
$r_{\text{S}}$ ( $\text{M}^{-1}\cdot\text{cm}^{-1}$ )		7.0 (0.4)

<sup>a</sup> The relative errors are presented in parentheses. The response ( $r$ ) corresponds to the extinction coefficient of each species. <sup>b</sup> The value for the rate constant  $k_4$  could not be estimated from the data registered upon hydrolysis of 0.5 and 2.5 mM penicillin G by Co(II)-substituted BcII. This was due to a low accumulation of the intermediate  $\text{ES}^2$  under those conditions. Hence, we fitted the 578 nm trace recorded upon reaction of 20 mM penicillin G with Co(II)-substituted BcII (Figure S6, Supporting Information). The value of  $k_4$  obtained from this fit was then fixed to fit the data corresponding to hydrolysis of 0.5 and 2.5 mM penicillin G. <sup>c</sup> The rate constants for formation and dissociation of MS ( $k_{+5}$  and  $k_{-5}$ ) could not be defined in the fit and were fixed to the values obtained for  $k_{+1}$  and  $k_{-1}$  when all four rate constants were allowed to float. When  $k_{+1}$  and  $k_{+5}$  were fixed to values reported for related systems,<sup>40,41</sup>  $k_{-1}$  and  $k_{-5}$  vary (with  $K_s$  almost constant), without any impact on the other rate constants or in the extinction coefficients reported in Table 1 (Figure S8, Supporting Information).

inactive mononuclear molecules would give rise to an active dinuclear form and apo enzyme can be ruled out since the dead time in the stopped-flow equipment (ca. 2 ms) is too short to allow for metal dissociation from one of the mono-Co(II) BcII populations ( $k_{\text{off}1} = 0.028 \text{ s}^{-1}$ ), and no lag phases were observed in samples with  $<1$  Co(II) equivalent. This evidence suggests that the branched mechanism considering a single active species is not able to account for the experimental data.

The best fits of the UV-vis data were obtained upon consideration of a branched kinetic pathway where both mono-Co(II) and di-Co(II) BcII are active (Model III, Scheme 1), both forms giving rise to catalytically competent enzyme-substrate complexes (MS and  $\text{ES}^1$ , respectively). The experimental data by Badarau and Page<sup>14</sup> can be accounted for by this model without assuming an inactive mono-Co(II) BcII species (Figure S10, Supporting Information). The rate constant that accounts for recovery of di-Co(II) BcII from  $\text{ES}^1$  ( $k_2$ ) was approximately 2-fold larger than the rate constant that describes recovery of mono-Co(II) BcII from MS ( $k_7$ ), see Table 1. Model III also includes a branched pathway with conversion of  $\text{ES}^1$  in  $\text{ES}^2$ . We analyzed the possibility that  $\text{ES}^2$  could represent an enzyme-product (EP) adduct. Addition of hydrolyzed penicillin G to resting-state Co(II)-BcII resulted in no changes in the absorption spectrum of this species, suggesting that the product does not tightly bind the enzyme. This is in agreement with

previous data from Bicknell and Waley, who demonstrated that  $\text{ES}^1$  and  $\text{ES}^2$  are different enzyme-substrate adducts.<sup>34</sup> Thus, penicillin hydrolysis leads directly to product release without significant intermediate accumulation or formation of a stable EP complex. This differs from the situation with Imipenem (see accompanying paper).

The changes in the intensity of the Cys  $\rightarrow$  Co(II) LMCT band at 330 nm could be fitted under the assumption that both enzyme-substrate complexes ( $\text{ES}^1$  and MS) contribute to this feature. Indeed, a fit to Model III predicts extinction coefficients for these contributions (Table 1) that are consistent with a LMCT band, therefore revealing that Cys221 is a metal ligand in both enzyme-substrate complexes. These results lead us to conclude that mono-Co(II)·DCH BcII is active, in contrast to the previous idea that mono-Co(II)·3H BcII could be the only active mononuclear species. Model III implies that binding of penicillin G to mono-Co(II) BcII gives rise to only one enzyme-substrate complex MS with the metal ion localized in the DCH site. This proposal requires a shift in the equilibrium between the two resting mononuclear enzyme species, mono-Co(II)·3H and mono-Co(II)·DCH, upon substrate binding (Scheme 2).

The assumption of a single active mononuclear species accumulating in Model III implies that the observed ligand field bands for MS correspond to the substrate-bound DCH site. Model III predicts an extinction coefficient at 560 nm of  $142 \text{ M}^{-1}\cdot\text{cm}^{-1}$  for MS (Figure S7, Supporting Information), which would correspond to a pentacoordinate DCH site. (The Co(II) ion at the DCH site in wt BcII displays an  $\epsilon_{520}$  of  $20 \text{ M}^{-1}\cdot\text{cm}^{-1}$ ,<sup>22</sup> while a DCH-localized mutant in which the His ligands of the 3H site were removed shows an  $\epsilon_{520}$  of  $40 \text{ M}^{-1}\cdot\text{cm}^{-1}$ ,<sup>43</sup> both interpreted as hexacoordinated Co(II).) Accordingly, the d-d bands observed for  $\text{ES}^1$  would correspond to the additive contribution of the spectra of Co(II) in the substrate-bound DCH site (similar to MS) and the spectrum of the substrate-bound 3H site. The estimated extinction coefficients from the fit at 560 nm for  $\text{ES}^1$  is  $271 \text{ M}^{-1}\cdot\text{cm}^{-1}$  (Figure S7, Supporting Information), which includes contributions of the 3H and DCH site which cannot be discerned from this fit. Subtraction of the value determined for MS gives an estimate of  $\epsilon_{560}$  of  $129 \text{ M}^{-1}\cdot\text{cm}^{-1}$  for the Co(II) ion at the substrate-bound 3H site, i.e., also pentacoordinate. These values, however, should be taken as approximate.

The results here presented and previous mechanistic studies available allow us to propose a branched catalytic mechanism that accounts for the spectral features discussed for the different enzyme species (Scheme 2). Penicillin G binding to the active site in di-Co(II) BcII is mostly driven by the interaction of the carboxylate group in the substrate with the Co(II) ion at the DCH site and with residue Lys224.<sup>44-47</sup> This metal-carboxylate interaction has been proposed to occur either by direct

(42) de Seny, D.; Prosperi-Meys, C.; Bebrone, C.; Rossolini, G. M.; Page, M. I.; Noel, P.; Frere, J. M.; Galleni, M. *Biochem. J.* **2002**, *363*, 687-696.

(43) Abriata, L. A.; Gonzalez, L. J.; Llarrull, L. I.; Tomatis, P. E.; Myers, W. K.; Costello, A. L.; Tierney, D. L.; Vila, A. J. *Biochemistry* **2008**, *47* (33), 8590-8599.

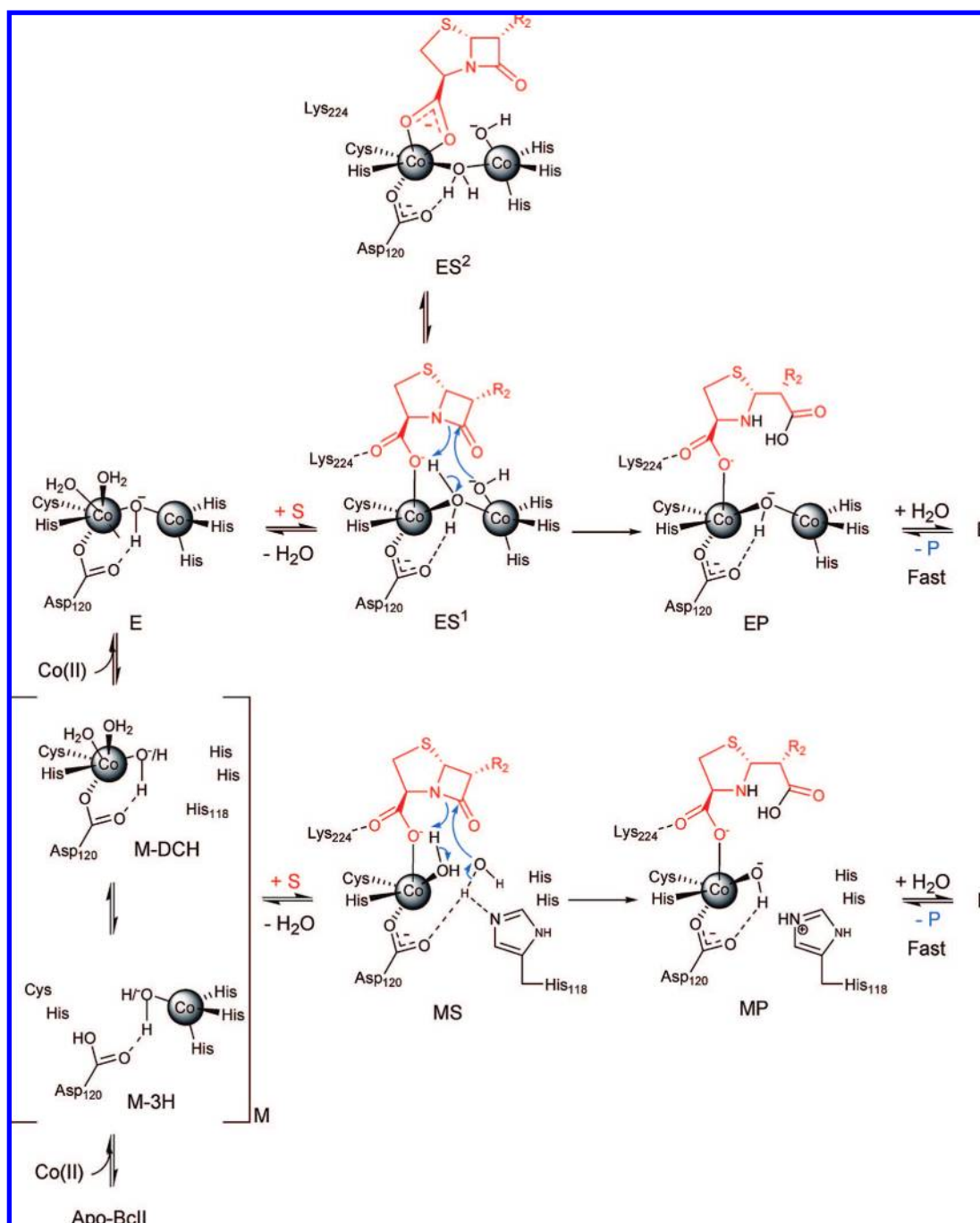
(44) Dal Peraro, M.; Vila, A. J.; Carloni, P.; Klein, M. L. *J. Am. Chem. Soc.* **2007**, *129* (10), 2808-2816.

(45) Gonzalez, J. M.; Medrano Martin, F. J.; Costello, A. L.; Tierney, D. L.; Vila, A. J. *J. Mol. Biol.* **2007**, *373* (5), 1141-1156.

(46) Oelschlaeger, P.; Schmid, R. D.; Pleiss, J. *Protein Eng.* **2003**, *16* (5), 341-350.

(47) Concha, N. O.; Janson, C. A.; Rowling, P.; Pearson, S.; Cheever, C. A.; Clarke, B. P.; Lewis, C.; Galleni, M.; Frere, J. M.; Payne, D. J.; Bateson, J. H.; Abdel-Meguid, S. S. *Biochemistry* **2000**, *39* (15), 4288-4298.



**Scheme 2.** Proposed Catalytic Mechanism for Penicillin G Hydrolysis Catalyzed by Co(II)-Substituted BcII<sup>a</sup>

<sup>a</sup> Note: While the Zn(II) ion at the DCH site is pentacoordinate according to the crystal structure, Co(II) would be hexacoordinate according to spectroscopic data. This difference can be accounted for by binding of a second water molecule to the Co(II) ion at this site as shown in E.

binding or mediated by a water molecule.<sup>45–48</sup> Our data do not allow us to distinguish between these two proposals, which are equally suitable to the herein proposed mechanism. In ES<sup>1</sup>, after substrate binding, the nucleophilic OH<sup>−</sup> detaches from the metal ion at the DCH site and the terminal H<sub>2</sub>O ligand at the DCH site now bridges the two metal ions.<sup>5</sup> In the model here proposed both Co(II) ions in the dinuclear site in the enzyme–substrate complex ES<sup>1</sup> have a pentacoordinate geometry, in agreement with the extinction coefficients estimated from Model III, as

discussed above. The bridging H<sub>2</sub>O molecule is the proton donor to the nitrogen atom of the  $\beta$ -lactam amide group.<sup>49</sup> A single chemical step is observed in all assayed conditions, revealing that the nucleophilic attack, the amide bond scission and protonation of the nitrogen atom of the  $\beta$ -lactam amide group are concerted. ES<sup>1</sup> rearranges to ES<sup>2</sup>, giving rise to a Co(II) ion with a lower extinction coefficient (Figure S7, Supporting Information), which can be interpreted as an increase in the coordination number. One possibility to account for this result

(48) Dal Peraro, M.; Vila, A. J.; Carloni, P.; Klein, M. L. *J. Am. Chem. Soc.* **2007**, *129* (10), 2808–2816.

(49) Dal Peraro, M.; Vila, A. J.; Carloni, P.; Klein, M. L. *J. Am. Chem. Soc.* **2007**, *129* (10), 2808–2816.

is to assume a bidentate carboxylate binding mode (Scheme 2). The substrate binding mode proposed for ES<sup>2</sup> would be nonproductive, in agreement with Model III. Thus far, this mechanism does not differ substantially from others already proposed, being limited to the dinuclear enzyme.<sup>5,50–54</sup>

At substoichiometric metal concentrations a significant amount of mononuclear enzyme is present that includes two populations with the Co(II) ion delocalized between the 3H and the DCH site, as already shown.<sup>15</sup> These two species were shown to be in fast equilibrium in mono-Cd(II) BcII with the exchange between both binding sites occurring on a time scale of 0.1–10  $\mu$ s.<sup>16</sup> The experimental evidence provided here reveals the accumulation of at least one active mononuclear intermediate (MS). The best possible fit of the kinetic data, based on the present knowledge of the system, leads us to suggest that this intermediate (MS) is substrate-bound mono-Co(II) BcII with the metal ion localized in the DCH site. Substrate binding to di-Co(II) BcII is driven by the interaction of the carboxylate group with the metal ion at the DCH site and with residue Lys224.<sup>45–47,55–57</sup> This binding mode can also take place in mono-Co(II)·DCH but is not possible in mono-Co(II)·3H. Therefore, penicillin binding to mono-Co(II)·DCH would shift the equilibrium between the two mono-Co(II) species in the unbound enzyme, leading to metal ion localization in the mononuclear enzyme–substrate adduct. We propose that the Co(II) ion at the DCH site in MS would be pentacoordinate, in agreement with the previously described interpretation of the extinction coefficients. The spectrum of MS (Figure S1, Supporting Information) closely resembles the one of Co(II)-substituted farnesyltransferase that adopts a 5-coordinate geometry with a Asp, Cys, and His protein ligand set,<sup>58</sup> supporting our assignment.

According to this model, in penicillin G hydrolysis catalyzed by mono-Co(II) BcII the nucleophile is expected to be a water molecule activated through hydrogen-bond interactions with residues in its near environment instead of a metal-bound solvent moiety. A similar mechanism has been proposed for the subclass B2 enzymes CphA and ImiS,<sup>36,59–61</sup> which are active only as mononuclear lactamases with a metal ion at the DCH site. In these cases it has been proposed that His118 or Asp120 would be involved in activating the attacking nucleophile. As observed for the dinuclear enzyme,  $\beta$ -lactam cleavage also proceeds through a single-step reaction in which amide bond scission is concerted with the nucleophilic attack and protonation of the

nitrogen atom. The model suggests that a H<sub>2</sub>O molecule coordinated to the metal ion in the DCH site would be the proton donor. Thus, neither the mononuclear nor the dinuclear forms lead to accumulation of a tetrahedral intermediate, in agreement with the absence of a conserved oxyanion hole in the active site of M $\beta$ LS.

As discussed before, we cannot definitively discard the presence of an active mono-Co(II)·3H species. In this case, the ligand field bands corresponding to MS would include the additive contribution from both metal sites, which cannot be discerned. We recently obtained two mononuclear mutants of BcII in which each of the metal binding sites was selectively removed, leading to inactive variants.<sup>43</sup> These data could be accounted for by assuming that only the dinuclear species is active or that the mononuclear forms can be active only if aided by other residues that would be metal ligands in the dinuclear species. The present data clearly favor the second hypothesis.

This mechanistic proposal reveals that B1 enzymes can be active in their mono- and dinuclear forms and that the mono-metallic species accumulating during turnover bears a metal ion bound to the DCH site. This view contrasts with the accepted proposal of the 3H site as the only catalytic one, which dates back to the first crystallographic structure of mono-Zn(II) BcII, which presented a single metal ion bound to the 3H site.<sup>19</sup> However, that structure was solved from crystals grown at low pH, and it has been shown that metal dissociation from BcII occurs at low pH with concomitant loss of activity.<sup>24</sup> The model here presented is derived from kinetic assays carried out in the presence of limiting metal concentrations, conditions that may be a good approximation to a metal-deprived *in vivo* situation.

The observation of similar spectral features at all Co(II)/BcII ratios might be also explained by assuming that the mono-Co(II)–DCH and mono-Co(II)–3H forms are equally (and independently) active. We would expect the mechanism of a mono-Co(II)–3H variant (involving a metal-activated nucleophile with no Zn<sup>2+</sup> ions to steer a water molecule for protonation of the N atom) and a mono-Co(II)–DCH species (which discards a metal-activated nucleophile and provides a Zn<sup>2+</sup> ion for substrate anchoring and help in delivering the proton) to be substantially different. Substrate binding is also expected to be very different for both mononuclear species.<sup>40</sup> Therefore, it is unlikely that both mononuclear species would have comparable catalytic efficiencies.

B2 lactamases, such as CphA and ImiS, were considered as atypical M $\beta$ LS based on the fact that they are exclusive carbenemases. We recently reported the characterization of a novel B3 enzyme, GOB, which is a broad spectrum lactamase, being active as a mononuclear enzyme with the metal ion localized in a metal binding site analogous to the DCH site. In GOB, the Zn(II) ion is bound to Asp120, His121, His263, and a water molecule<sup>62</sup> and would play a similar catalytic role as the one here proposed for the DCH site in mononuclear BcII without the need of a metal-activated nucleophile. These results are also in line with the observation that engineering a more buried position for this metal site in BcII results in a largely impaired lactamase activity.<sup>5,29,45,63</sup>

The present results can be extended to the native metal ion, Zn(II), and other substrates. The much larger difference between

(50) Garrity, J. D.; Carenbauer, A. L.; Herron, L. R.; Crowder, M. W. *J. Biol. Chem.* **2004**, *279* (2), 920–927.

(51) Wang, Z.; Fast, W.; Benkovic, S. J. *Biochemistry* **1999**, *38* (31), 10013–10023.

(52) Spencer, J.; Read, J.; Sessions, R. B.; Howell, S.; Blackburn, G. M.; Gamblin, S. J. *J. Am. Chem. Soc.* **2005**, *127* (41), 14439–14444.

(53) Dal Peraro, M.; Vila, A. J.; Carloni, P.; Klein, M. L. *J. Am. Chem. Soc.* **2007**, *129* (10), 2808–2816.

(54) Park, H.; Brothers, E. N.; Merz, K. M. *J. Am. Chem. Soc.* **2005**, *127*, 4232–4241.

(55) Dal Peraro, M.; Vila, A. J.; Carloni, P.; Klein, M. L. *J. Am. Chem. Soc.* **2007**, *129* (10), 2808–2816.

(56) Dal Peraro, M.; Vila, A. J.; Carloni, P. *Proteins* **2004**, *54* (3), 412–423.

(57) Dal Peraro, M.; Llarrull, L. I.; Rothlisberger, U.; Vila, A. J.; Carloni, P. *J. Am. Chem. Soc.* **2004**, *126* (39), 12661–12668.

(58) Huang, C. C.; Casey, P. J.; Fierke, C. A. *J. Biol. Chem.* **1997**, *272* (1), 20–23.

(59) Garau, G.; Bebrone, C.; Anne, C.; Galleni, M.; Frere, J. M.; Dideberg, O. *J. Mol. Biol.* **2005**, *345* (4), 785–795.

(60) Xu, D.; Xie, D.; Guo, H. *J. Biol. Chem.* **2006**, *281* (13), 8740–8747.

(61) Simona, F.; Magistrato, A.; Vera, D. M.; Garau, G.; Vila, A. J.; Carloni, P. *Proteins* **2007**, *69* (3), 595–605.

(62) Moran-Barrio, J.; Gonzalez, J. M.; Lisa, M. N.; Costello, A. L.; Peraro, M. D.; Carloni, P.; Bennett, B.; Tierney, D. L.; Limansky, A. S.; Viale, A. M.; Vila, A. J. *J. Biol. Chem.* **2007**, *282* (25), 18286–18293.

(63) Crisp, J.; Conners, R.; Garrity, J. D.; Carenbauer, A. L.; Crowder, M. W.; Spencer, J. *Biochemistry* **2007**, *46* (37), 10664–10674.

$K_D$ (mononuclear) and  $K_D$ (dinuclear) for Zn(II)<sup>11</sup> compared to Co(II) is only expected to modify the differences in the initial concentrations of mononuclear and dinuclear species at each metal/enzyme ratio, but the mechanism might be similar. However, the metal ion delocalization at substoichiometric metal contents is common to Co(II), Cd(II), and Zn(II).<sup>11,12,15,16</sup> Metal localization upon substrate binding would be driven by the interaction of the carboxylate moiety of penicillin with the metal ion at the DCH site. Even considering that Zn(II) and Co(II) may display different metal binding preferences, this electrostatic interaction should be equally important for shifting an equilibrium both for Co(II) and Zn(II), and the same localization event could be predicted for Zn(II). This metal ion–carboxylate interaction has been reported for complexes of the dinuclear B3 Zn(II)–L1 enzyme with the product of hydrolysis of moxalactam<sup>46</sup> and of the mononuclear B2 enzyme CphA with the product of hydrolysis of biapenem.<sup>49</sup> Thus, there is strong evidence supporting the relevant role of this interaction for all bicyclic  $\beta$ -lactam substrates. In the accompanying paper, we show that this phenomenon is also valid for carbapenems.<sup>64</sup>

The finding that the DCH site is able to give rise to an active lactamase suggests that the Zn2 site is a common feature to all subclasses of metallo- $\beta$ -lactamases being present in B1, B2, and

B3 enzymes and playing a similar role. This proposal is a starting point for the design of inhibitors based on transition-state analogues, which might be effective against all M $\beta$ Ls. These results also prompt the need of RFQ-EXAFS studies on the native enzyme to transfer the present mechanistic model to the Zn form.

**Acknowledgment.** This work was supported by grants from ANPCyT and HHMI to A.J.V. L.I.L. was a recipient of a doctoral fellowship from CONICET. A.J.V. and M.F.T. are Staff members from CONICET, and A.J.V. is also an International Research Scholar of the Howard Hughes Medical Institute.

**Supporting Information Available:** Equilibrium concentrations of the different enzyme species in the resting state; electronic spectra of MS and ES1; fit of the 578 nm data to Model I; fit of the 578 nm data to Model II; fit of the 578 nm data to Model IV; fit of the 578 nm data to Model V; fit of the 578 nm data obtained upon hydrolysis of 20 mM penicillin G by Co(II)–BcII to Model III; fit of the 560 nm data to Model III; analysis of the effect of fixing  $k_{+5}$  and  $k_{+1}$  on Model III to different values; fit of the 578 and 330 nm to Model III modified to consider both mononuclear forms of BcII as active species; simulation of a pre-steady-state experiment. This material is available free of charge via the Internet at <http://pubs.acs.org>.

JA801168R

(64) Tioni, M. F.; Llarrull, L. I.; Poeylout-Palena, A. A.; Martí, M. A.; Saggiu, M.; Periyannan, G. R.; Mata, E. G.; Bennett, B.; Murgida, D. H.; Vila, A. J. *J. Am. Chem. Soc.* **2008**, *130*, 15852–15863, following paper in this issue.